Laser Remelting of Plasma-Sprayed Yttria Partially Stabilized Zirconia Coatings

J.H. Ouyang and Xiaodong Li

(Submitted 31 January 2000)

A plasma-sprayed 8 wt.% yttria partially stabilized zirconia coating doped with 3 wt.% SiO_2 was remelted by laser. The microstructure of the as-sprayed and laser-remelted coatings was characterized by scanning electron microscopy (SEM), electron probe microanalysis (EPMA), transmission electron microscopy (TEM), and x-ray diffraction (XRD). The effect of laser remelting on the hardness, wear resistance, and thermal shock resistance of the coatings was also studied. The laser-remelted coating consists of fine solidification grains without the presence of pores and cracks. The elements are uniformly distributed in the laser-remelted coating. Nontransformable tetragonal (t') phase is predominant in the laser-remelted coating with a small amount of cubic phase. Laser remelting greatly enhanced the hardness, wear resistance, and thermal shock resistance of the coatings, and should find more applications.

Keywords laser remelting, mechanical properties, microstructure, plasma-sprayed yttria partially stabilized zirconia coatings

1. Introduction

Plasma-sprayed thermal barrier coatings (TBCs) have been widely used to provide thermal insulation to components operating in the hot regions of diesel, turbine, and engines.[1,2] Using TBCs, the surface temperature of hot components can be reduced as much as 100 to 200 °C, thus improving the efficiency of the engines and their lifetime.[3–6] A typical TBC uses 8 wt.% yttria partially stabilized zirconia (YPSZ), which produces a nonequilibrium and high yttria content tetragonal phase during plasma spraying due to rapid cooling.[5] ZrO_2 coatings also have been used as wear protective coatings for hot components, such as sealed rings, which require not only better thermal barrier properties but also higher wear resistance. Wear can change the size of sealed rings, thus resulting in failure of the rings. The present paper focuses on the wear protective coatings for hot components. The primary problem with plasma spraying for such coatings is the high porosity, with many micropores, microcracks, and nonbonded interface areas between lamellae existing in the coatings, which reduces thermal insulation and corrosion performance.[5,6,7] To densify plasma-sprayed coatings, post-treatment by laser remelting has been developed. Laser remelting can seal open pores, enhance coating strength and chemical homogeneity, and develop metallurgical bonding at the coating-substrate interface, producing strengthened coating adhesion.[6,7] Laser remelting can also offer greater flexibility, such as a short processing time, less thermal distortion, and fewer microstructure changes to the substrate.[7,8]

Laser remelting of ZrO_2-based ceramic TBCs may lead to the formation of cracks in the coatings due to the thermal stress caused by the thermal expansion mismatch between the ceramic coating and substrate.[6,9] Studies have shown that the addition of aluminia, silica, and titania powders to the ZrO_2-based coatings can greatly reduce the thermal stresses in the coatings.[5,10] Although work has been done on the laser remelting of TBCs, the microstructure and mechanical properties of the laser-remelted coatings are still, to a large extent, unknown. Superalloys, as high-temperature materials, have been widely used as substrates for plasma-spray coatings. However, using plasma-spray coatings to protect steel components operating at high temperatures is attracting more attention. In this paper, a plasma-sprayed 8 wt.% yttria partially stabilized ZrO_2 coating doped with 3 wt.% SiO_2 on UNS S42000 steel was remelted by laser. The microstructure and mechanical properties of the laser-remelted coatings were studied. The phase transformation during laser remelting is also discussed in conjunction with the changes in mechanical properties.

2. Experimental Procedures

Twelve millimeter thick UNS S42000 steel plates were used as coating substrates. The composition (wt.%) of the UNS S42000 steel was 13Cr, 0.8Mn, 0.4Si, 0.35C, and the balance Fe. Eight weight percent Y_2O_3 partially stabilized ZrO_2 powders with a particle size of about 60 μm were used as coating materials. Three weight percent SiO_2 powders with a particle size of about 22 μm were mixed into the YPSZ powders to reduce the thermal stresses in the coatings. An R750-C plasma-spraying equipment (Plasma Technik AG, Zuerich, Switzerland) was used in this study. Coatings were deposited by atmospheric plasma spray. Before spraying, the substrates were grit blasted and then cleaned in an alcohol ultrasonic bath. To reduce the thermal stress mismatch between the coating and substrate, a 20 to 50 μm thick bond layer was first coated on the substrate

J.H. Ouyang, Fraunhofer Institute for Material and Beam Technology, D-01277, Dresden, Germany, and School of Materials Science and Engineering, Harbin Institute of Technology, Harbin 150001, People's Republic of China; and **Xiaodong Li**, School of Materials Science and Engineering, Harbin Institute of Technology. Contact e-mail: li.233@osu.edu.

Table 1 Plasma spray parameters used for depositing YPSZ coatings

Parameter	ZrO_2 ceramic powder	NiCoCrAlY
Arc voltage	62 kV	60 kV
Arc current	500 A	460 A
Primary gas, flow rate	Ar, 30 L/min	Ar, 40 L/min
Auxiliary gas, flow rate	H_2, 10 L/min	H_2, 10 L/min
Powder feed rate	40 g/min	75 g/min
Spraying distance	160 mm	180 mm

using NiCoCrAlY powders with a particle size of about 30 μm. The composition (wt.%) of the NiCoCrAlY powders was analyzed to be 19.41Co, 15.3Cr, 7.83Al, 0.76Y, and the balance Ni. The mixed powders of YPSZ and SiO_2 were sprayed on the bond layer. The plasma spray parameters are shown in Table 1. The YPSZ and NiCoCrAlY powders used in this study were supplied by Beijing Research Institute of Mining and Metallurgy (Beijing).

Laser remelting was carried out using a Rofin-Sinar (Hamburg, Germany) RS1700SM 2.1 kW continuous wave CO_2 laser. The laser was operated in a transverse electromagnetic transmission electron microscope (TEM_{10}) mode with a defocused beam of about 3 mm diameter. Argon gas shielding with a shielding box was used to protect the melt pool from the outside atmosphere and reduce the surface defects. The laser operating parameters were 0.4 to 0.9 kW laser power, 3 mm beam diameter, and 8 to 45 mm/s traverse speed.

The microstructure of the as-sprayed and laser-remelted coatings was characterized using a Hitachi (Tokyo, Japan) S-570 scanning electron microscope and a Philips CM12 (Philips Electronic Instruments Corporation, Mahwah, NJ) operated at 120 kV. The cross-sectional specimens for scanning electron microscopy (SEM) observations were cut from the coated specimens using an abrasive wheel flooded with water. Before cutting, an epoxy adhesive was put onto the coating sides to ensure the coating's integrity during cutting. The cut specimens were polished using 180 to 1600 grit abrasive SiC papers, followed by 1 μm diamond particle suspension, and then chemically etched in a 3% Nital for substrate observation and a 100% hot hydrofluoric acid for coating observation. For transmission electron microscope (TEM) specimens, coatings of about 0.5 mm thickness were first cut parallel to the surface. The cut sides were ground on SiC papers to the specimen thickness of 50 μm. Then the 50 μm thick plates were glued to a glass slide and cut by a ceramic drill of 3 mm internal diameter flooded with water. The 3 mm discs were ground, dimpled, and thinned by ion milling.

The structure of the PYSZ powders, as-sprayed, and laser-remelted coatings was analyzed using a Siemens (Munich, Germany) D5000 x-ray diffractometer with 40 kV operating voltage and Co K_α radiation. A labeling program with a 2θ scanning speed of 2 deg $\cdot$ min^{-1} was used in the range $20° < 2\theta < 100°$. A step scanning program with a 2θ scanning rate of 0.02 deg $\cdot$ s^{-1} was employed to determine the peak intensities of different phases.

The hardness of the as-sprayed and laser-remelted coating specimens was measured using a microhardness tester. The wear resistance of the as-sprayed and laser-melted coatings was studied using a pin-on-ring wear tester. The ring of the wear couple was made of WC-8 wt.% Co hard alloy with a hardness value of 1120 $HV_{0.1}$. The pin samples were 10 $\times$ 4 mm in cross section. Before the wear test, the ring and coating surfaces were mechanically polished to the roughness of about 60 μm. The normal load was 50 N and the sliding speed was 1.05 ms^{-1}. The total sliding distance was 180 m. For more details about the wear test, please see Ref 11. The thermal shock resistance test was carried out in an electric furnace. The specimen was first heated to 1000 °C and held for 20 min. Then the heated specimen was taken out of the furnace and cooled by water or air to room temperature. This thermal cycle process was repeated until coating spallation was found under an optical microscope. The thermal cycle number was used to evaluate the thermal shock resistance. The data of hardness, wear resistance, and thermal shock test were based on the average values of five samples.

3. Results and Discussion

Figure 1 shows the surface morphologies of the as-sprayed and laser-remelted coatings. The as-sprayed coating surface is rough and porous with many cracks, whereas the laser-remelted coating surface is smooth and dense with few small cracks. The remelted region exhibits a resolidified structure with a striated morphology (Fig. 1c). The striated morphology is attributed to solidification shrinkage. During cooling, the transformation from the cubic phase to the nontransformable tetragonal phase may relieve solidification shrinkage.

Figure 2 shows the cross-sectional SEM images of the as-sprayed coating. The as-sprayed coating exhibits a lamellar structure with many partially melted and unmelted powder particles and pores. The interface between the coating and substrate is very rough. The pores and cracks are considered as defects in such coatings.[5,6,7] There exist strong coating/substrate interfacial stresses because of the thermal contraction mismatch between the metal substrate and ceramic coating. The rough coating/substrate interface induces localized stresses. These interfacial residual stresses could lead to coating delamination and buckling in practical applications.

Figure 3 shows the cross-sectional SEM images of the laser-remelted coating. The remelted coating consists of fine solidification columnar/dendritic grains of about 10 μm in width and about 50 to 100 μm in length. No pores were observed in the remelted coating. The energy-dispersive x-ray analysis (EDXA) results indicate that elements are uniformly distributed in the remelted coating. Below the remelted coating was a 50 mm thick bond layer. The interfaces between the remelted coating and the bond layer and the substrate are sharp. The bond layer was diluted by the stainless steel. The EDXA results show that the composition (wt.%) of the bond layer is 61.18Fe, 24.03Ni, 5.87Cr, 4.64Co, 2.32Al, 1.77Zr, 0.08Si, and 0.11Y. The microstructural constituents of the bond layer were analyzed to be γ dendrites, γ', and chromium carbide in the interdendritic areas.

Figure 4 shows the x-ray diffraction (XRD) spectra of the original YPSZ powders and the as-sprayed coating. The original YPSZ powders consist of (at.%) 29% cubic (c), 37% tetragonal (t), and 34% monoclinic (m) phases. The metastable tetragonal (t') phase is predominant in the as-sprayed coating with a small

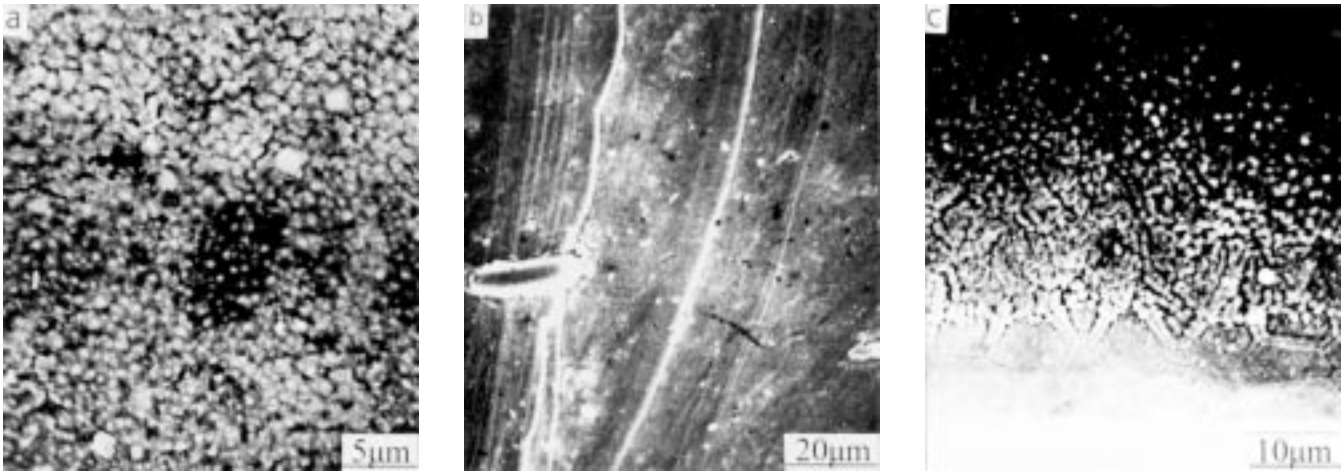

Fig. 1 Surface morphologies of the as-sprayed and laser-remelted coatings: (**a**) as-sprayed coating, (**b**) laser-remelted coating, and (**c**) interface between the laser-remelted region and the surrounding as-sprayed region

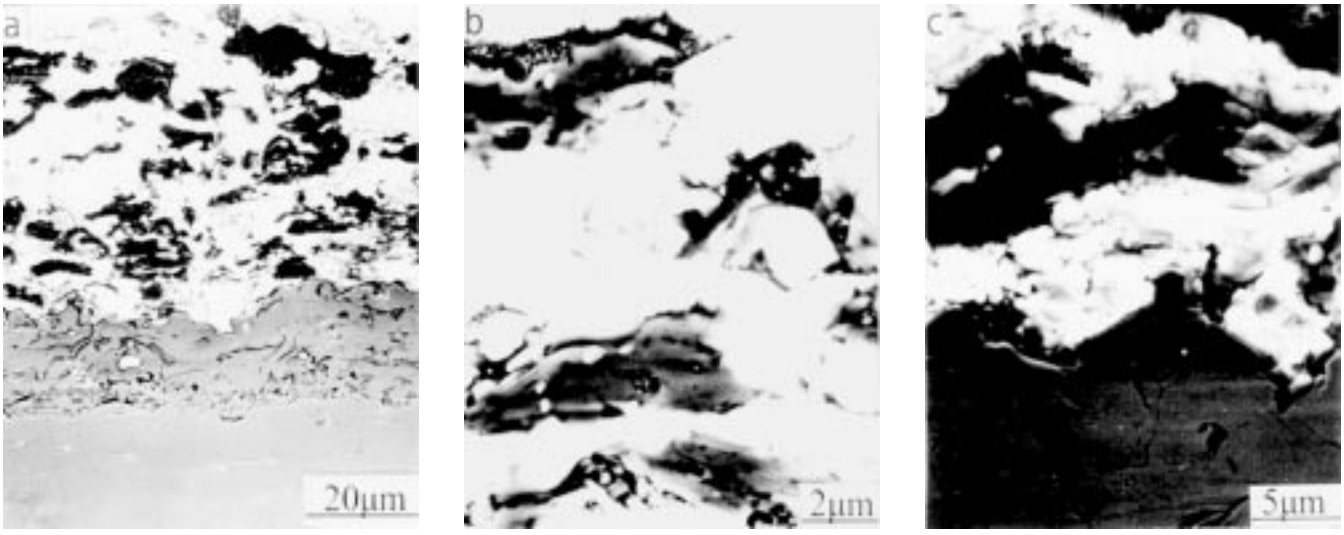

Fig. 2 Cross-sectional SEM images of the as-sprayed coating: (**a**) as-sprayed coating, (**b**) high-magnification image of the as-sprayed coating, and (**c**) interface between the as-sprayed coating and bond layer

amount of *c* (6 at.%) and *m* (4 at.%) phases. It is believed that the *c* and *m* phases resulted from incomplete melting of the powders during spray. No silica peaks were found, indicating the SiO_2 powders were completely melted during spraying.

Figure 5 shows the XRD spectra of the laser-remelted coating. Nontransformable tetragonal t' phase is predominant in the laser-remelted coating with a small amount of *c* phase. The presence of the t' phase is attributed to the rapid cooling during laser remelting. The t' phase is the product of an athermal displasive transformation that occurs when the *c* phase containing 5 to 7 mol.% yttria is quenched.[9] No *m* phase peaks were found, indicating that the *m* phase was melted during laser remelting.

Figure 6 shows the TEM images of the as-sprayed coating. The equiaxed t' grain is about 0.6 μm, consisting of tetragonal variants in the form of plates approximately 0.05 μm wide. The EDXA results demonstrate that yttrium is uniformly distributed in the t' phase and the yttrium content in the t' phase is close to that in the YPSZ powders. A small amount of *m* phase with a low yttrium content was also observed at the interfaces between the unmelted particles in the as-sprayed coating (Fig. 6b).

The microstructure of the as-sprayed and laser-melted coatings was studied by TEM. Selected area diffraction techniques were used to determine various phases of interest in the coatings. Figure 7 shows the TEM images of the laser-remelted coating. Many fine t' precipitates were also observed with different tetragonal variants. The EDXA results demonstrated that the t' phase has a high yttrium content, close to that of the initial powder. The bright structure at the grain boundary region shown in Fig. 7 (b) has high silicon, but low zirconium and yttria contents. These grain boundary regions are silica rich and act as thermal stress relieving additions in the coatings.

Microhardness measurements were carried out on the cross sections of the as-sprayed and laser-remelted coatings. The hardness of the laser-remelted coating is 1420 to 1538 $HV_{0.1}$,

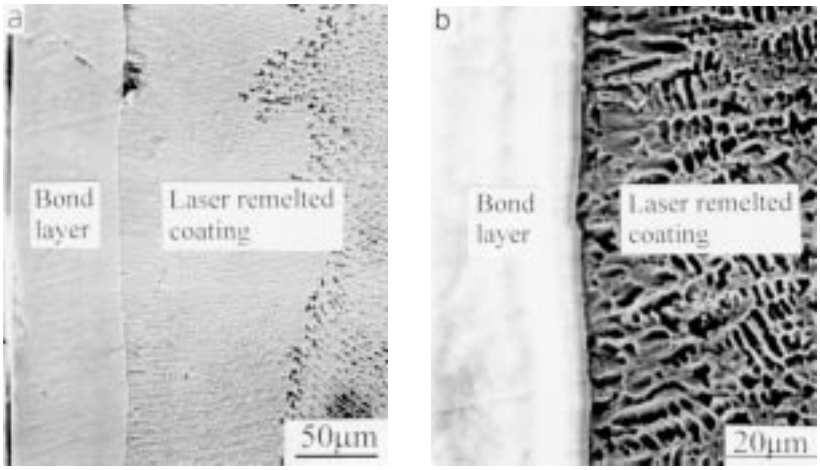

Fig. 3 Cross-sectional SEM images of the laser-remelted coating: (**a**) laser-remelted coating and (**b**) interface between the laser-remelted coating and bond layer

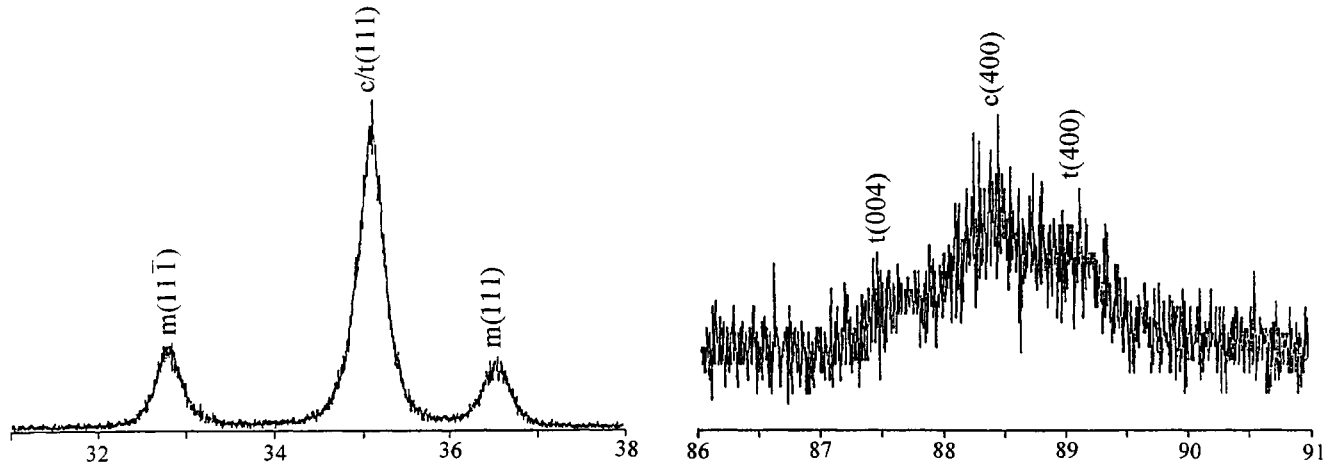

(**a**)

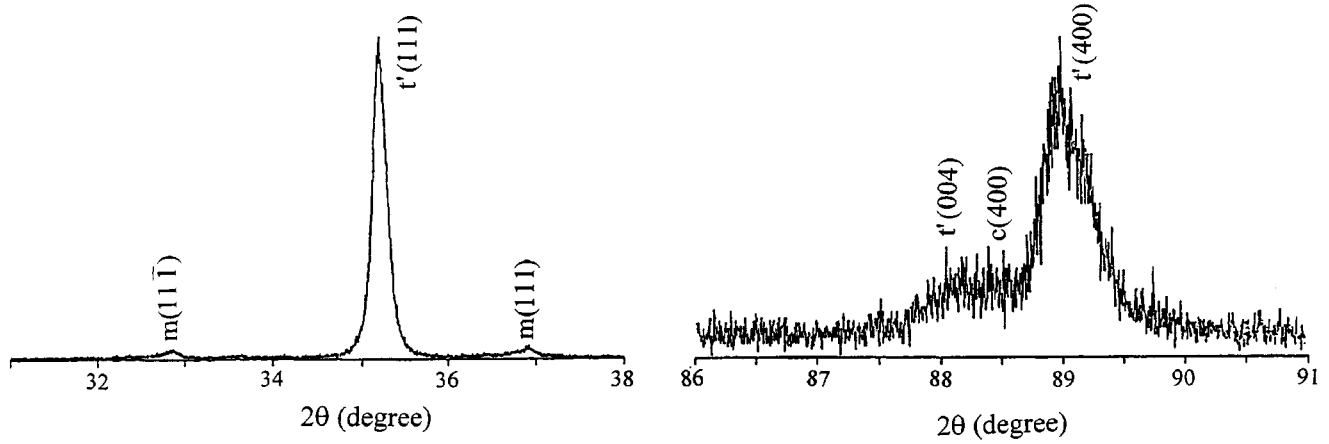

(**b**)

Fig. 4 XRD spectra of (**a**) the original YPSZ powders and (**b**) the as-sprayed coating

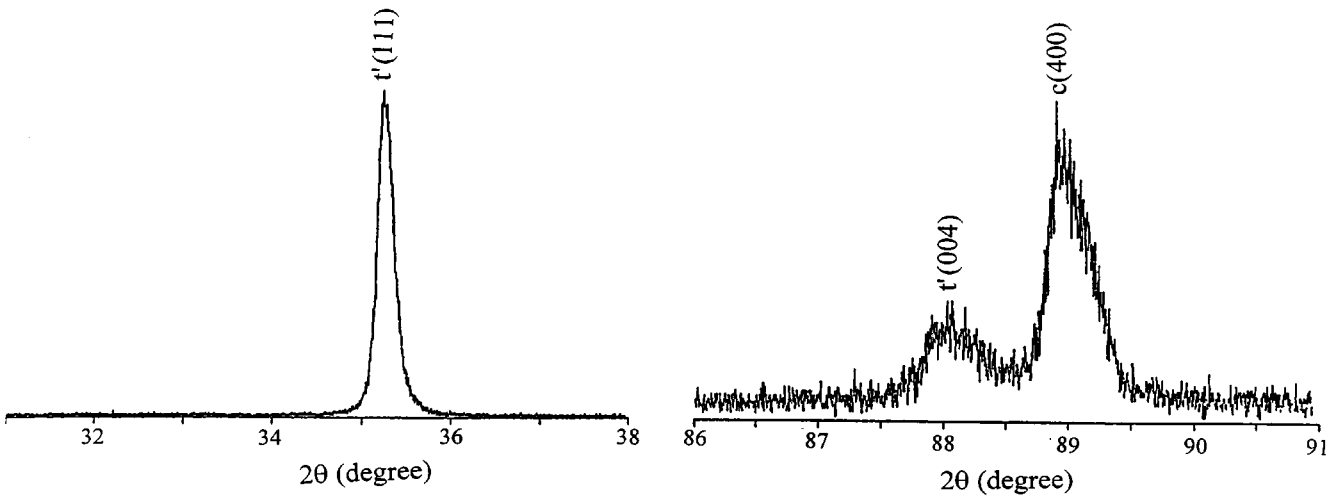

Fig. 5 XRD spectra of the laser-remelted coating

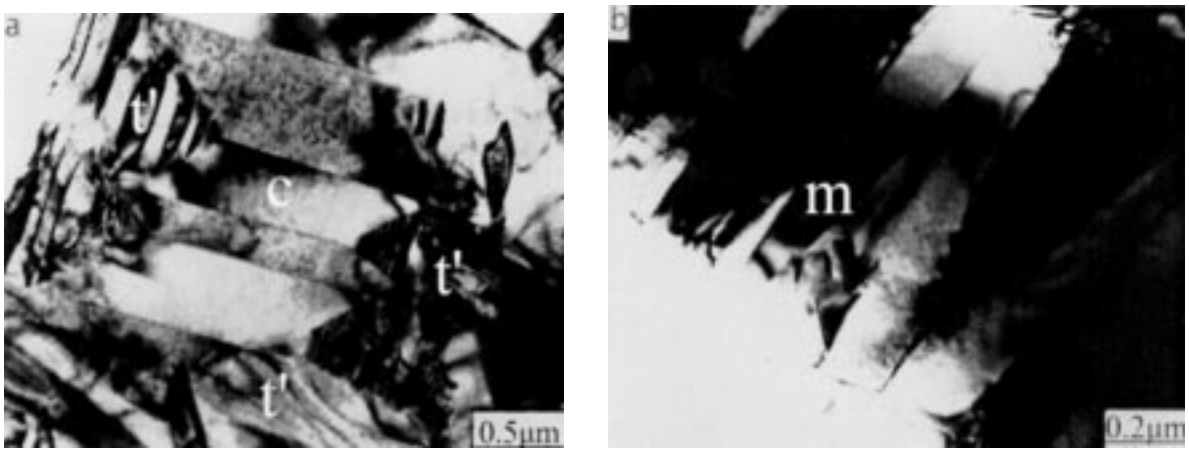

Fig. 6 TEM images of the as-sprayed coating: (**a**) t' phase and (**b**) m phase at the interface between the YPSZ particles

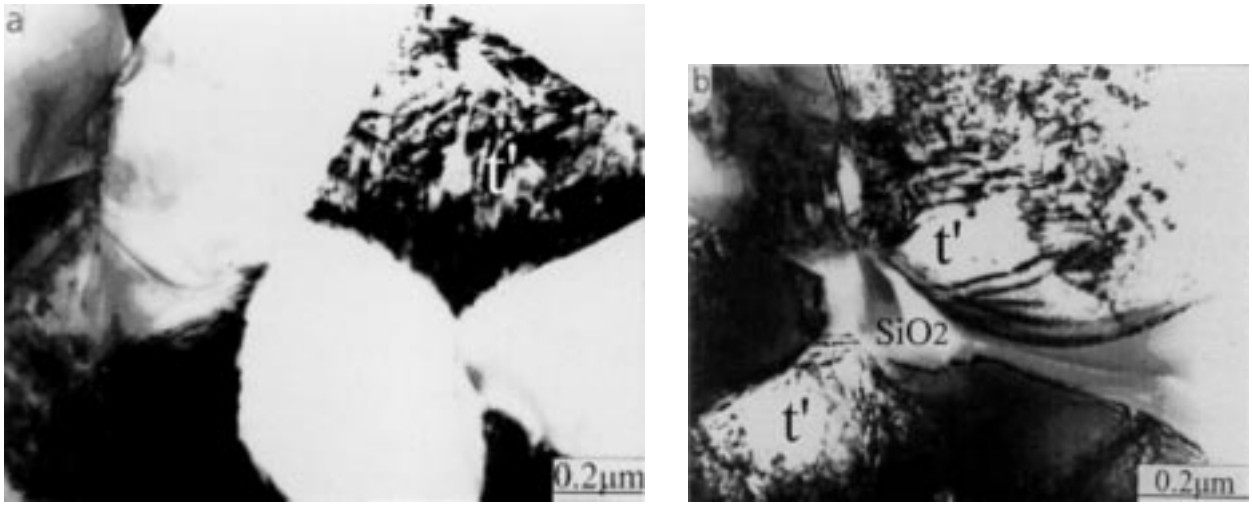

Fig. 7 TEM images of the laser-remelted coating: (**a**) t' phase and (**b**) interfacial silica-rich structure

Table 2 Thermal cycle number of the as-sprayed, laser-remelted coatings held at 1000 °C for 20 min in an electric furnace

	Plasma-sprayed coating	Laser remelted coating
Water cooling	1	2
Air cooling	19	35

which is much higher than the hardness of the as-sprayed coating (731 to 844 $HV_{0.1}$). The hardness of the laser-overlapped regions is 1287 to 1489 $HV_{0.1}$.

The wear resistance of the as-sprayed and laser-remelted coatings was evaluated by the weight loss method. The wear resistance of the laser-remelted coating is two times higher than that of the as-sprayed coating. The enhanced hardness and wear resistance of the laser-remelted ZrO_2 coatings are mainly attributed to the absence of pores and cracks and the fine resolidified structure.

The laser remelting greatly enhanced the thermal shock resistance of the as-sprayed coating. The laser-remelted coating shows an enhanced resistance to thermal cycle shock as compared with the as-sprayed coating, as shown in Table 2. The high thermal shock resistance is attributed to the strong metallurgical bonding between the laser-remelted coating and substrate and the improvement of strain accommodation by laser remelting.[7]

4. Conclusions

Laser remelting greatly improves the microstructure and mechanical properties of YPSZ coatings. The laser-remelted coating consists of fine solidification grains without presence of pores and cracks. The elements are uniformly distributed in the laser-remelted coating. The nontransformable tetragonal phase is predominant in the laser-remelted coating with a small amount of *c* phase. The laser-remelted coating exhibits higher hardness, wear resistance, and thermal shock resistance than the as-sprayed coating. The laser-remelting technique should find more applications.

Acknowledgment

One of the authors, Dr. J.H. Ouyang, gratefully acknowledges the partial financial support of the Alexander von Humboldt Foundation and the Chinese Aerospace Foundation.

References

1. R.A. Miller: *Surf. Coating Technol.*, 1987, vol. 30 (1), pp. 1-11.
2. R. Taylor, J.R. Brandon, and P. Morrell: *Surf. Coating Technol.*, 1992, vol. 50 (2), pp. 141-49.
3. E. Vandehaar, P.A. Molian, and M. Baldwin: *Surf. Eng.*, 1988, vol. 4 (2), pp. 159-72.
4. B.C. Wu, E. Chang, C.H. Chao, and M.L. Tsai: *J. Mater. Sci.*, 1990, vol. 25 (2A), p. 1112.
5. H.C. Chen, E. Pfender, and J. Heberlein: *Thin Solid Films*, 1998, vol. 315 (1-2), pp. 159-69.
6. H.L. Tsai, P.C. Tsai, and D.C. Tu: *Mater. Sci. Eng. A*, 1993, vol. 161 (1), pp. 145-55.
7. Y. Fu, A.W. Batchelor, H. Xing, and Y. Gu: *Wear*, 1997, vol. 210 (1-2), pp. 157-64.
8. G.Y. Liang and T.T. Wong: *Surf. Coating Technol.*, 1997, vol. 89 (1-2), pp. 121-26.
9. K.M. Jasim, R.D. Rawlings, and D.R.F. West: *Surf. Coating Technol.*, 1992, vol. 53 (1), pp. 75-86.
10. A. Petitbon, D. Guignot, U. Fischer, and J.M. Guillemot: *Mater. Sci. Eng. A*, 1989, vol. 121 (2), pp. 545-48.
11. X. Li, Y. Wang, and J. Liu: *Wear*, 1991, vol. 150 (1-2), pp. 59-65.